

JPL Document D-71066

TECHNOLOGY DEVELOPMENT FOR EXOPLANET MISSIONS

Phase-Induced Amplitude Apodization (PIAA) Technology
Development; Milestone #2 Whitepaper

Instrument Tip-Tilt Control Demonstration at the sub-Milli-arcsecond level

Olivier Guyon, PI

Glenn Schneider, Laird Close, Brian Kern, Andreas Kuhnert, Amir Giveon, Laurent Pueyo, Stuart Shaklan, Ruslan Belikov, Eugene Pluzhnik, Frantz Martinache, Thomas Greene, Kerri Cahoy, Robert Vanderbei, Jeremy Kasdin, Stephen Ridgway, Domenick Tenerelli, Robert Woodruff, Alan Duncan, Tony Hull

16 September 2011

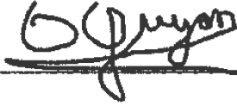
National Aeronautics and Space Administration

Jet Propulsion Laboratory
California Institute of Technology

Copyright 2011. All rights reserved.

Approvals

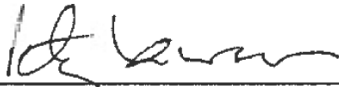
Released by



Olivier Guyon
Principal Investigator

Sept 16, 2011

Approved by



Peter R. Lawson
Exoplanet Program Chief Technologist, JPL

9/19/2011



Marie Levine
Exoplanet Exploration Technology Manager, JPL

9/19/2011



Michael Devirian
Exoplanet Exploration Program Manager, JPL

9/19/2011



Douglas Hudgins
Exoplanet Exploration Program Scientist, NASA HQ

9/20/11



Lia LaPiana
Exoplanet Exploration Program Executive, NASA HQ

Sept 20, 2011

TABLE OF CONTENTS

1. Objective.....	1
2. Introduction.....	1
2.1. The Coronagraphic Low Order Wavefront Sensor (CLOWFS).....	1
2.2. Tip-tilt control requirements for direct imaging of exoplanets.....	2
3. Milestone description: Tip-Tilt control to $0.01 \lambda/D$, Calibration of residual Tip-Tilt to $0.003 \lambda/D$	5
3.1. Milestone definition.....	5
3.2. Description of PIAA laboratory configuration.....	6
3.3. Differences between Laboratory Demonstration and Flight.....	7
4. Computation of the Metric.....	8
4.1. Definitions.....	8
4.2. Tip-tilt measurement with the CLOWFS: initial calibration of the CLOWFS response.....	8
4.3. Tip-tilt measurement with the CLOWFS: pointing jitter.....	9
4.4. Tip-tilt measurement with the CLOWFS: calibration residual.....	9
5. Success Criteria.....	10
6. Certification Process.....	11
6.1 Milestone Certification Data Package.....	11
7. References.....	11
Appendix A: Low Order Wavefront Sensor (LOWFS) demonstration with PIAA coronagraph system at the Subaru Telescope Testbed.....	13
Appendix B: The Pupil mapping Exoplanet Coronagraphic Observer (PECO).....	15
Appendix C: Pointing control on PECO.....	17

1. Objective

In support of technology development for NASA's Exoplanet Exploration Program (ExEP), this whitepaper explains the purpose of the second Milestone for Phase-Induced Amplitude Apodization (PIAA) coronagraphy, specifies the methodology for computing the milestone metric, and establishes the success criteria against which the milestone will be evaluated.

2. Introduction

The Technology Milestones serve to gauge the developmental progress of technology for a space-based mission that would detect and characterize exoplanets, and the mission's readiness to proceed from pre-Phase A to Phase A. Completion of the milestones is to be documented in a report by the Principal Investigator, reviewed by the ExEP Technology Assessment Committee, and approved by the Program and NASA HQ.

This document describes the second milestone of the ongoing development effort for a PIAA coronagraph. The first milestone is a demonstration of a monochromatic contrast of 1×10^{-9} with PIAA optics [1]. The second milestone, the topic of this whitepaper, is a demonstration of pointing stability and calibration:

“Demonstrate 0.01 λ/D RMS pointing jitter stability and 0.003 λ/D pointing calibration at the coronagraph focal plane mask over a continuous 1-hr time period”

This milestone will demonstrate the sub-milli-arcsecond tip-tilt control required for achieving and maintaining high contrast (1×10^{-9} raw contrast) at small inner working angles ($< 2 \lambda/D$). This is being specifically applied to a PIAA coronagraph [2-11]. The approach for accomplishing this milestone is to implement and operate a dedicated sensor, the Coronagraphic Low-Order Wave-Front Sensor (CLOWFS) on the existing PIAA coronagraph table which is currently in the vacuum Micro-Arcsecond Metrology (MAM) chamber at NASA Jet Propulsion Laboratory (JPL).

We commit to release into the public domain the details of algorithms and analysis methods/codes used for the NASA-funded lab performance validation activity described in this paper. This release will be done by publication to public domain scientific journal(s) and release of code/data into publicly accessible website(s) to a level of detail sufficient for independent implementation and validation of our approach.

2.1. The Coronagraphic Low Order Wavefront Sensor (CLOWFS)

The CLOWFS uses light reflected by the coronagraphic focal plane to measure low order aberrations. The very central part (from center to radius $\sim 1 \lambda/D$) of the focal plane mask is made opaque, while the area immediately around it (annulus from radius $\sim 1 \lambda/D$ to $\sim 2 \lambda/D$) is reflective. This combination of opaque and reflective coatings produces an annular

region in the focal plane which is reflected and fed into the CLOWFS camera. This design allows higher measurement precision than would be possible with a purely reflective mask. A camera acquires defocused images of the mask, and its response (images) is a linear function of the tip and tilt values. A detailed technical description of the CLOWFS is available through a previous refereed publication [12] and in Appendix A, to which the interested reader is referred. The CLOWFS is an essential part of the pointing control strategy for the PECO mission concept [13-17]. Appendix B provides an overview of the PECO mission concept, and its pointing control strategy is described in Appendix C. This approach, of including the CLOWFS signal for accurate pointing calibration, is relevant to any coronagraph delivering high contrast images at small inner working angle.

A coronagraph testbed validating the CLOWFS was built and operated at the Subaru Telescope. This testbed demonstrated 2×10^{-7} raw contrast in monochromatic light at $1.65 \lambda/D$ separation in air [18] and a $10^{-3} \lambda/D$ closed loop pointing control [12], corresponding to 0.1 mas on the 1.4-m diameter PECO mission concept telescope. The Subaru testbed effort was discontinued in early 2009 and its final results have been compiled in a publication [18]. Appendix A also provides an overview of results obtained on the Subaru Testbed.

The milestone described in this whitepaper is an extension of previous work and has as its goal the laboratory demonstration of instrument pointing measurement and control with a particular internal coronagraph architecture. The demonstration will be performed to a level of accuracy suitable for direct imaging of Earth-like planets with a medium-size space telescope, provided that tip-tilt variations are the only sources of error in the system.

This work is being carried out with an award from the NASA Research Opportunities in Space and Earth Sciences (ROSES) solicitation on Strategic Astrophysics Technology, and in particular is subtopic on Technology Development for Exoplanet Missions.

2.2. Tip-tilt control requirements for direct imaging of exoplanets

We describe in this section the rationale for the milestone requirements. As detailed in this section, the amount of residual tip-tilt required for this milestone is not derived from a mission-specific contrast error budget. It is instead established from fundamental principles, requiring that the residual tip-tilt is equal to the angular size of a Sun-like star at 10pc. Meeting this requirement thus ensures that, even with the most aggressive coronagraph designs (smallest inner working angle), the coronagraph raw-contrast performance is not limited by residual tip-tilt jitter, as coronagraph leaks due to the angular size of the central star will then be larger than those due to tip-tilt jitter. For less aggressive coronagraph designs, that operate with larger inner working angles, the requirements given in this milestone are therefore conservative. The completion of this milestone provides lab environment test validation data for any internal coronagraph instrument concept that chooses to use hardware component technology, control systems, and software that are traceable to our team's CLOWFS approach, in mission concepts that have no more stressing conditions or operational environments that our PECO mission concept technology development will later address.

Although control of all low-order aberrations is challenging on a high contrast imaging system, tip and tilt are likely to be the modes with the most jitter, as vibrations and telescope pointing can

easily induce large tip-tilt errors. Cross-talk between tip-tilt and other low-order modes in the LOWFS, as predicted from numerical simulations, is small to moderate (<10%). The combined effect of the expected dominance of tip-tilt and small/moderate cross-talk is that our LOWFS estimates of tip-tilt are likely to be good (to probably about 1% or better) representations of the real tip and tilt. We however realize that without detailed analysis of cross-talk between tip-tilt and other low-order modes in the LOWFS, it is difficult to be quantitative about the level of cross-talk from other modes that contribute to our measurement, especially because we have little knowledge of how strongly other modes vary in time. In-depth study of cross-talk between modes is beyond the scope of this work, and we assume for this milestone that tip-tilt are the only disturbances in the coronagraph system, and that the LOWFS measurement is not affected by other modes.

2.2.1 Instrument contrast requirement for direct imaging of Earth-like planets

In visible light, an Earth analog around a Sun-like star is approximately 10^{10} times fainter than its parent star (the exact value is a function of planet phase and albedo). With a medium-sized (4-m diameter or smaller) telescope operating at the diffraction limit, the planet image is superimposed on a background due to zodiacal light and exozodiacal light at the $\sim 10^{-9}$ contrast level (10 times brighter in surface brightness than the planet image peak surface brightness). The instrument raw contrast (level of starlight scattered on the planet image) must be sufficiently low to allow detection and characterization of the planet in the presence of photon noise from the combined instrument (residual speckle halo) + astrophysical (zodiacal + exozodiacal light) sources. For this milestone, we adopt the following requirement:

(a) PHOTON NOISE LIMITED PERFORMANCE: Tip-tilt must be controlled well enough to ensure that the scattered light surface brightness due to residual tip-tilt errors is equal or less than the scattered light due to astrophysical sources, corresponding to a raw contrast requirement of 1×10^{-9} .

We note that this requirement is somewhat arbitrary (planets can still be detected and characterized with larger levels of scattered light if the total exposure time is increased). The required photon-noise limited exposure time scales linearly with total background surface brightness: while there is little benefit in reducing instrumental raw contrast below the astrophysical background, the mission science performance decreases rapidly as instrumental background increases above the astrophysical background level.

In addition to observing with the photon noise limit described above, the instrument must also allow signal-to-noise ratio (SNR) of 10 detection of an Earth analog in an observation of sufficient duration to average down photon noise below $1/10^{\text{th}}$ of the planet flux:

(b) CALIBRATION LIMITED PERFORMANCE: Residual tip-tilt errors must be calibrated sufficiently well to offer a 1×10^{-11} instrument contrast limit after removal of known instrument residuals and calibration using available wavefront sensing signals.

2.2.2 Importance of inner working angle for direct imaging of exoplanet

New high performance coronagraph concepts can theoretically deliver the performance required for direct imaging and spectroscopic characterization of Earth-like planets around stars with medium-size telescopes (in the 2 to 4-m range). To do so, it is essential that these coronagraphs combine small inner working angle (IWA) and high throughput. For a given telescope diameter, the IWA at the $\sim 1 \times 10^{-9}$ raw contrast level drives the number of stars around which Earth-like planets can be imaged, and is therefore the single most important instrument performance parameter (although other parameters, such as throughput and ability to maintain the high contrast across a usable spectral bandwidth are also very important). Since the number of exoplanets that can be imaged is primarily a function of IWA, it scales as IWA^{-3} (volume around the observer within which a certain type of planet is IWA-accessible): reducing the IWA from $2 \lambda/D$ to $1 \lambda/D$ produces an eight-fold increase in exoplanets that could be imaged. **Low IWA coronagraphs are therefore key to the science return of an exoplanet-imaging mission.**

2.2.3 New low-IWA coronagraphs

While the coronagraphs baselined for TPF-C FB1 [19] had an IWA of approximately $4 \lambda/D$, recent advances have shown that significantly smaller IWA can be achieved. Among the new coronagraph concepts, the PIAA and Optical Vortex can deliver the required 10^{-9} raw contrast at $2 \lambda/D$ with nearly full throughput, and efforts are currently being deployed in the laboratory to demonstrate this level of performance. The newly developed Phase-induced amplitude apodization complex mask coronagraph (PIAACMC) concept [11], a hybrid including a PIAA coronagraph, an Apodized Pupil Lyot Coronagraph (APLC) and a Roddier-type phase mask coronagraph, can be designed to deliver 10^{-10} contrast at $0.64 \lambda/D$ around an unresolved point source [11].

2.2.4 IWA, tip-tilt jitter and stellar angular size

While the small-IWA coronagraph concepts are on paper extremely attractive, achieving these performance levels requires exquisite control and knowledge of tip-tilt and other low order aberrations. With large-IWA coronagraphs, the wavefront quality requirement per mode for a 10^{-9} raw contrast is $\sqrt{2 \text{ contrast}} \lambda/\pi \sim 7 \text{ pm RMS}$ for mid-spatial frequencies¹ but is considerably relaxed for low order aberrations, as the light they scatter is still behind the coronagraph focal plane mask. On small-IWA coronagraphs, this is no longer the case, and the wavefront quality requirement for low order aberration becomes closer to the mid-spatial frequency requirement.

2.2.5 Tip-tilt RMS jitter requirement

The ultimate limit to coronagraph performance for small IWA coronagraphs is set by angular size of the star, which we assume in this document is 1 mas (Sun-like star at 10 pc). Optimal performance is reached when the coronagraph IWA is reduced until it becomes limited by stellar angular size at the 1×10^{-9} raw contrast level. **Regardless of coronagraph type (PIAA, Optical Vortex or other) or telescope diameter, the requirement for control of tip-tilt is therefore equal to the stellar angular size:** there is no incentive to reduce residual tip-tilt jitter below the stellar angular radius, as it will not result in improved contrast. There is however a strong performance loss if residual tip-tilt jitter is larger than stellar angular size, as it will either preclude

¹ This value is obtained by considering modes corresponding to individual speckles in the focal plane (=sine wave in phase in the pupil plane) and allocating the same 1×10^{-9} contrast for each speckle.

the use of small-IWA coronagraphs, or lead to significant light leakage in a small-IWA coronagraph. The examples illustrated in Table 1 are for a star with an angular diameter of 1.0 mas, that thus requires an RMS tip-tilt jitter no larger than its angular radius of 0.5 mas.

2.2.6 Tip-tilt calibration requirement

While tip-tilt jitter requirement is set by the level of scattered light in the coronagraphic image (which, as described above, must not exceed the contribution due to the stellar angular size), the tip-tilt contribution to the final coronagraphic image needs to be calibrated to approximately 1/10 of that level to ensure that planets can be detected at a SNR=10 if present at the same raw contrast level as the coronagraphic leaks. The complex amplitude contribution of pointing errors in the focal plane scales at least linearly with tip-tilt angle (depending on the working contrast, PIAA coronagraph design, and tip-tilt amplitude, the scaling law can be linear or quadratic), and the light intensity therefore scales as the square of the tip-tilt jitter, or to a higher power of tip-tilt jitter. For small tilt-tilt errors, we can therefore write:

$$\text{Coronagraph leak} \sim \text{pointing error}^\alpha$$

With $\alpha > 2$. Assuming a quadratic law between tip-tilt angle and coronagraphic leak (intensity) is therefore conservative for the goal of this milestone: calibration in the image to 1/10th of the coronagraphic leak due to stellar angular diameter requires tip-tilt calibration to at most 1/sqrt(10) of the stellar angular radius. To define the tip-tilt calibration requirement for this milestone, we adopt the conservative assumption that $\alpha = 2$.

For the examples in Table 1, the stellar angular radius is 0.5 mas, and therefore the tip-tilt must be calibrated to 0.17 mas. Table 1 illustrates the requirements as a function of telescope diameter.

Telescope diameter ($\lambda = 0.5\mu\text{m}$)	Allowable Tip-tilt jitter (RMS)	Tip-tilt calibration / knowledge requirement (averaged over observation)
1.4-m telescope	0.5 mas = 0.0068 λ/D	0.17 mas = 0.0023 λ/D
2-m telescope	0.5 mas = 0.0097 λ/D	0.17 mas = 0.0032 λ/D
4-m telescope	0.5 mas = 0.0194 λ/D	0.17 mas = 0.0065 λ/D

Table 1: Pointing jitter and calibration requirements as a function of telescope diameter. The values shown in this table ensure that a small-IWA coronagraph is limited by stellar angular size rather than pointing errors. For this milestone, we adopt the requirements for a 2-m diameter telescope observing a 1mas diameter star at $\lambda = 0.5\mu\text{m}$.

3. Milestone description: Tip-Tilt control to 0.01 λ/D , Calibration of residual Tip-Tilt to 0.003 λ/D

3.1. Milestone definition

“Demonstrate 0.01 λ/D RMS pointing jitter stability and 0.003 λ/D pointing calibration at the coronagraph focal plane mask over a continuous 1-hr time period”

The milestone will be achieved using a Phase-Induced Amplitude Apodization coronagraph system and a Coronagraphic Low Order Wavefront Sensor (CLOWFS). As detailed in Section 2, the level of pointing jitter and calibration for this milestone are what is required to ensure that, on a 2-m telescope, any coronagraph design (even with aggressively low IWA) will be limited by stellar angular size before it becomes limited by tip-tilt errors.

3.2. Description of PIAA laboratory configuration

The optical configuration for the milestone will be identical to the current PIAA MAM configuration (Figure 1), to which the CLOWFS will be added.

Figure 1 shows the PIAA bench optical layout. The light source is located at the bottom right corner of the figure, and illuminates mirror PIAA M1 with a diverging spherical wave. Mirror PIAA M2 focuses the light to a first focal point, after which the beam is collimated by an off-axis parabola (OAP M3). In the collimated space between M3 and M4 is a plane conjugated to PIAA M2, where a selection of classical apodizers and stops can be interchanged. A second OAP (M4) then focuses the light to a second focus (F2), after which the diverging beam is recollimated by OAP M5. The wavefront is controlled by a single 32x32 actuator deformable mirror, located in collimated space after OAP M5. The mirror is manufactured by Xinetics and converts voltages into displacement of individual actuators bonded to a thin reflective mirror. OAP M7 focuses the beam on the focal plane mask (opaque disk of metal deposited by microlithography on a clear glass substrate), after which OAP M8 collimates the beam. Mirror M9 is a flat in collimated space, and OAP M10 focuses the light on the camera.

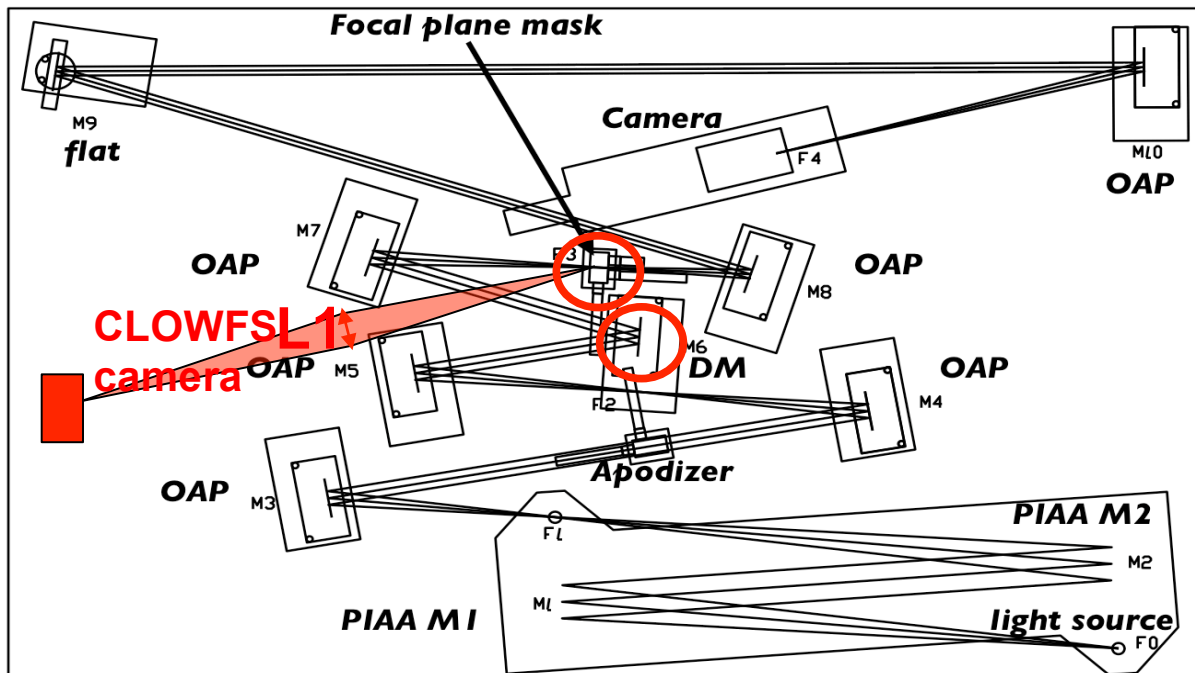


Figure 1: Optical layout of the PIAA testbed in the MAM chamber. Hardware modifications to implement the CLOWFS are shown in red, and include (1) replacing the focal plane mask by a reflective annulus, (2) lens L1 to produce the CLOWFS image, (3) a camera to capture the CLOWFS image, and (4) actuation of the DM mount to control instrument tip-tilt.

The CLOWFS will be implemented by (1) replacing the current focal plane mask with a partially reflective focal plane mask which sends part of the starlight in the direction between OAP M5 and OAP M7, (2) adding between OAP M5 and OAP M7 a refractive re-imaging optical system, (3) adding the CLOWFS camera behind OAP M5 and OAP M7, on the left edge of the bench shown in Figure 1, and (4) actuating the DM mount to allow tip-tilt control.

3.3. Differences between Laboratory Demonstration and Flight

Environment

For this milestone, we do not plan to introduce vibrations in the system, and we will only correct the inherent disturbance on the bench. Early tests have shown that these disturbances are at the $0.04 \lambda/D$ level over a 1 hr time period. Our proposed experiment will use a CCD camera for acquisition of CLOWFS frames, operating at a frame rate of approximately 4 Hz (improvements in the frame rate may occur). The light level and loop parameters will be set to optimize performance: the light source will be sufficiently bright to avoid excessive readout noise in the CLOWFS, and the loop gain will be set to obtain the smallest tip-tilt residual. Our experiment does therefore not consist of a test in realistic conditions (spacecraft disturbance, photon flux, space-qualified CLOWFS hardware), which are design-specific (telescope diameter, throughput, filter bandwidth, spacecraft design, orbit, etc...). We will however document the conditions under which our experiment is performed (source flux, PSD of inherent disturbances, loop gain, camera frame rate) to facilitate future comparison with realistic space environment and telescope/instrument design.

Our milestone will be achieved in a laboratory environment with a light source rather than the focal plane of a telescope at the input of the instrument, and qualifies as a "Component and/or breadboard validation in laboratory environment". Upon completion of this milestone, the CLOWFS will be at Technology Readiness Level 4, defined as:

"Following successful "proof-of-concept" work, basic technological elements must be integrated to establish that the "pieces" will work together to achieve concept-enabling levels of performance for a component and/or breadboard. This validation must be devised to support the concept that was formulated earlier, and should also be consistent with the requirements of potential system applications. The validation is "low-fidelity" compared to the eventual system: it could be composed of ad hoc discrete components in a laboratory."

We note that the particular hardware and software implementation approach adopted by our team may not be suitable for use in a space-based instrument, and that including space environment related constraints (power, mass, computing constraints, resistance to launch) will require further advances in maturity.

4. Computation of the Metric

4.1. Definitions

Tip-tilt and pointing error are here defined at the coronagraph focal plane mask location. This is the location where such aberrations lead to coronagraphic leaks, and consequently, this is where tip-tilt must be controlled.

Tip-tilt will be **measured relative to a zero point** which is constant for the duration of the experiment. This zero point is adopted by choosing a nominal CLOWFS image I_0 . All CLOWFS images I are then decomposed as :

$$I = I_0 + x I_x + y I_y \quad (\text{equ 4.1})$$

with I_x and I_y the response of the CLOWFS to tip and tilt motions (see section 4.2 for a description of how these two images are obtained), and x and y the measured tip and tilt values (angles). The values x and y in equation 4.1 are computed through a least-square fit of the pixels of each image, where the sum is with respect to the pixel number :

$$\text{residual} = \text{SUM} [(I - (I_0 + x I_x + y I_y))^2]$$

over a disk centered on the CLOWFS image. We have been using a 15 pixel diameter disk in our preliminary tests, but its radius may be adjusted to optimize performance. We may also apply SNR-based weights to individual pixels to improve performance.

A CLOWFS image, or CLOWFS frame is an array of pixel values read from the CLOWFS CCD camera, with the following low-level processing performed: bias subtraction and normalization to unity pixel values sum (in order to avoid sensitivity to source flux variations).

4.2. *Tip-tilt measurement with the CLOWFS: initial calibration of the CLOWFS response*

Tip-tilt will be measured by the CLOWFS according to equ 4.1. The calibration of the CLOWFS response is required to perform this measurement, and consists of measuring I_0 , I_x and I_y (images), and is performed by actuating the DM tip-tilt mount by known offsets and measuring the corresponding CLOWFS response. The calibration images will be measured as follows:

STEP 1: After alignment of the coronagraph and CLOWFS, acquire a CLOWFS image I (which may consist of an average of several individual frames to reduce noise). This image is I_0 , the CLOWFS reference image

STEP 2: Offset the DM tip-tilt mount by a known tip value x . Acquire a new CLOWFS image I (which may consist of an average of several individual frames to reduce noise). The calibration image I_x is computed as follows:

$$I_x = (I - I_0) / x$$

STEP 3: Offset the DM tip-tilt mount by a known tilt value y (and no offset in x). Acquire a new CLOWFS image I (which may consist of an average of several individual frames to reduce noise). The calibration image I_y is computed as follows:

$$I_y = (I-I_0)/y$$

Steps 1-3 should be performed for several positive and negative values of x and y covering all four quadrants of XY-space in order to assess the precision and range of validity of equation 4.1.

4.3. Tip-tilt measurement with the CLOWFS: pointing jitter

Measurement of the tip-tilt jitter will be made in closed loop with the CLOWFS continuously measuring tip and tilt according to equ 4.1. The measured values for tip and tilt are then used to actively control tip-tilt by actuating a correction device, which can be the position of the light source or the Deformable Mirror tip-tilt angle. For this measurement, no tip-tilt actuation other than the commands issued by the tip-tilt correction loop is issued.

The measurement sequence is therefore as follows:

STEP #1: set iteration number $i=0$

STEP #2: measure the values (x_i, y_i) of x and y for iteration i according to equ 4.1, using a CLOWFS image

STEP #3: Apply tip-tilt offset $(-g x_i, -g y_i)$ to tip-tilt actuated device (source or DM), where g is the loop gain $(0 < g < 1)$, chosen to optimize loop performance

STEP #4: increment i, go back to STEP #2

The tip and tilt RMS jitter values are computed as follows:

$$\sigma_x = \sqrt{\langle x_i^2 \rangle_i} ; \sigma_y = \sqrt{\langle y_i^2 \rangle_i} \quad (\text{equ 4.2})$$

Where x_i and y_i are the measured tip and tilt values for iteration i, and the average is to be performed over the duration of the experiment ($i=0..i_{\max}$).

4.4. Tip-tilt measurement with the CLOWFS: calibration residual

The tip and tilt calibration residual values are defined as the average tip-tilt values during the measurement and can be computed from the same set of data as follows:

$$\bar{\delta}_x = \langle x_i \rangle_i ; \bar{\delta}_y = \langle y_i \rangle_i \quad (\text{equ 4.3})$$

Where $(\langle x_i \rangle_i ; \langle y_i \rangle_i)$ are the CLOWFS measured tip tilt values averaged over the duration of the experiment ($i=0..i_{\max}$). To validate that the CLOWFS calibration residual meets our requirement, we require:

$$\sqrt{\bar{\delta}_x^2 + \bar{\delta}_y^2} < 0.003 \lambda/D \quad (\text{Requirement 1})$$

This requirement is necessary but not sufficient to ensure that the calibration requirement is met: since the average tip-tilt values are measured from the same signal as used for the active correction, there is a significant risk that $\bar{\delta}_x^2 + \bar{\delta}_y^2$ do not represent the true tip-tilt values at the $0.003 \lambda/D$ accuracy level. We therefore must also independently verify the validity of the CLOWFS signal at the $0.003 \lambda/D$ accuracy level.

This will be done in a separate measurement by adding a known tip-tilt error signal (a sine wave in voltage on the high voltage line to one of the tip-tilt actuators) and estimating its amplitude from the CLOWFS measurements. A function generator, wired in series with the analog output to the piezo tip-tilt actuators on the DM mount, will be used to introduce a ~ 0.1 Hz error signal. Its amplitude will be reconstructed from Fourier analysis of the x_i and y_i values measured by the CLOWFS. For this test, the CLOWFS can run in closed or open loop (if running in closed loop, the measured values need to be added to the corrections to recover the open-loop equivalent measurement).

The CLOWFS estimate of the sine wave error signal must be accurate to $0.003 \lambda/D$ (Requirement 2)

Our calibration residual requirement will be met only if both requirements are satisfied.

5. Success Criteria

The following are the required elements of the milestone demonstration. Each element includes a brief rationale.

5.1. The duration of the experiment for each of the measurements should be at least 1hr and correspond to at least 1000 CLOWFS samples. Both constraints must be satisfied: the measurement should therefore last more than 1hr if the frame rate is insufficient to obtain 1000 samples within 1hr, and the measurement will consist of more than 1000 samples if the frame rate is sufficiently fast to obtain the 1000 samples in less than 1hr.

Rationale: *This ensures that a sufficiently large number of measurement points are used toward computing the jitter and calibration residuals.*

5.2. A residual jitter of $0.01 \lambda/D$ or smaller shall be achieved as defined in Sec. 4.3. This requirement is on the radial jitter value: the quadratic sum of the jitter in x and y must be $0.01 \lambda/D$ or smaller.

Rationale: *This provides evidence that the coronagraph leak due to tip-tilt errors is smaller than the contribution of stellar angular size.*

5.3. A residual calibration residual of $0.003 \lambda/D$ or smaller shall be achieved as defined in Sec. 4.4. This requirement is on the radial calibration residual value: the quadratic sum of the calibration residual in x and y must be $0.01 \lambda/D$ or smaller.

Rationale: *This ensures that calibration of tip-tilt errors is sufficient to recover planets 10 times fainter than the 1×10^{-9} contrast raw scattered light due to stellar angular size, zodiacal light and exozodiacal light.*

5.4. Elements 5.1 – 5.3 must be satisfied on three separate occasions with a reset of the CLOWFS (discarding calibration and re-calibrating the CLOWFS) between each demonstration.

Rationale: *This provides evidence of the repeatability of the contrast demonstration. The CLOWFS reset between data sets ensures that the three data sets can be considered as independent and do not represent an unusually good configuration that cannot be reproduced. There is no required interval between demonstrations; subsequent demonstrations can begin as soon as prior demonstrations have ended.*

6. Certification Process

The Principal Investigator will assemble a milestone certification data package for review by the Exoplanet Exploration Program and its Technology Advisory Committee. In the event of a consensus determination that the success criteria have been met, the Program will submit the findings of the TAC, together with the certification data package, to NASA HQ for official certification of milestone compliance. In the event of a disagreement between the Program and the TAC, NASA HQ will determine whether to accept the data package and certify compliance or request additional work.

6.1 Milestone Certification Data Package

The milestone certification data package will contain the following explanations, charts, and data products.

- 6.1.1. A narrative report, including a discussion of how each element of the milestone was met, an explanation of each image or group of images, appropriate tables and summary charts, and a narrative summary of the overall milestone achievement.
- 6.1.2. Calibrated images of the CLOWFS calibration frames, raw frames, and x and y values.
- 6.1.3. Values for the tip and tilt jitter, and tip and tilt calibration residual for each of the 3 sets of data required to reach the milestone.

7. References

- [1] Phase-Induced Amplitude Apodization (PIAA) Technology Development; Milestone #1 Whitepaper
- [2] Guyon, O. "Phase-induced amplitude apodization of telescope pupils for extrasolar terrestrial planet imaging," *A&A*, v.404, p.379-387 (2003)
- [3] "[Two-Mirror Apodization for High-Contrast Imaging](#)" Traub, Wesley A.; Vanderbei, Robert J. *ApJ*, 599, 695 (2003)
- [4] "[Pupil Mapping in Two Dimensions for High-Contrast Imaging](#)" Vanderbei, Robert J.; Traub, Wesley A. *ApJ*, 626, 1079 (2005)
- [5] "Exoplanet Imaging with a Phase-induced Amplitude Apodization Coronagraph. I. Principle" Guyon, O., Pluzhnik, E.A., Galicher, R., Martinache, F., Ridgway, S.T., Woodruff, R.A., *ApJ*, 622, 744-758 (2005)
- [6] "Exoplanet Imaging with a Phase-Induced Amplitude Apodization Coronagraph. II. Performance", Martinache, F., Guyon, O., Pluzhnik, E.A., Galicher, R., Ridgway, S.T., *ApJ*, 639, 1129-1137, (2006)
- [7] "[Diffraction Analysis of Two-dimensional Pupil Mapping for High-Contrast Imaging](#)" Vanderbei, Robert J. *ApJ*, 636, 528 (2006)

- [8] "Exoplanet Imaging with a Phase-Induced Amplitude Apodization Coronagraph. III. Diffraction Effects and Coronagraph Design", Pluzhnik, E.A., Guyon, O., Ridgway, S.T., Martinache, F., Woodruff, R.A., Blain, C., Galicher, R., ApJ, 644, 1246-1257, (2006)
- [9] Guyon, O., Pluzhnik, E.A., Kuchner, M.J., Collins, B., Ridgway, S.T., "Theoretical Limits on Extrasolar Terrestrial Planet Detection with Coronagraphs", ApJ Suppl, 167, 81 (2006)
- [10] Lozi, J., Martinache, F., Guyon, O. "Phase-Induced Amplitude Apodization on centrally obscured pupils: design and first laboratory demonstration for the Subaru Telescope pupil", PASP, Volume 121, Issue 885, pp. 1232-1244 (2009)
- [11] "High Performance PIAA Coronagraphy with Complex Amplitude Focal Plane Masks", ApJ, 192, 220, (2010) http://www.naoj.org/staff/guyon/publications/2009-10_PIAACMC.pdf
- [12] Guyon, O., Matsuo, T., Angel, R., "Coronagraphic Low Order Wavefront Sensor: Principle and Application to a Phase-Induced Amplitude Coronagraph", ApJ, 693, pp 75-84 (2009)
- [13] PECO website: <http://caao.as.arizona.edu/PECO>
- [14] PECO report to astro2010: http://caao.as.arizona.edu/PECO/PECO_Report.pdf
- [15] PECO science requirements document: http://caao.as.arizona.edu/PECO/PECO_SRD.pdf
- [16] PECO design reference mission: http://caao.as.arizona.edu/PECO/PECO_DRM.pdf
- [17] PECO Technology Development Plan: http://caao.as.arizona.edu/PECO/PECO_techdev.pdf
- [18] Guyon, O.; Pluzhnik, E.A.; Martinache, F; Totems, J.; Tanaka, S.; Matsuo, T.; Blain, C.; Belikov, R. "High Contrast Imaging and Wavefront Control with a PIAA Coronagraph: Laboratory System Validation", PASP (2010), http://www.naoj.org/staff/guyon/publications/2009-11-07_PIAA_labexp.pdf
- [19] Levine, M. et al., "Levine, M., et. al (2009) Terrestrial Planet Finder – Coronagraph (TPF-C) Flight Baseline Mission Concept", white paper provided to the 2010 Decadal Survey (2009)

Appendix A: Low Order Wavefront Sensor (LOWFS) demonstration with PIAA coronagraph system at the Subaru Telescope Testbed

The low order wavefront sensor concept and implementation are described in [12]. We summarize here results obtained with the LOWFS on the Subaru PIAA system and discuss their relevance to both the MAM PIAA experiment and the PECO pointing control strategy described in Appendix C.

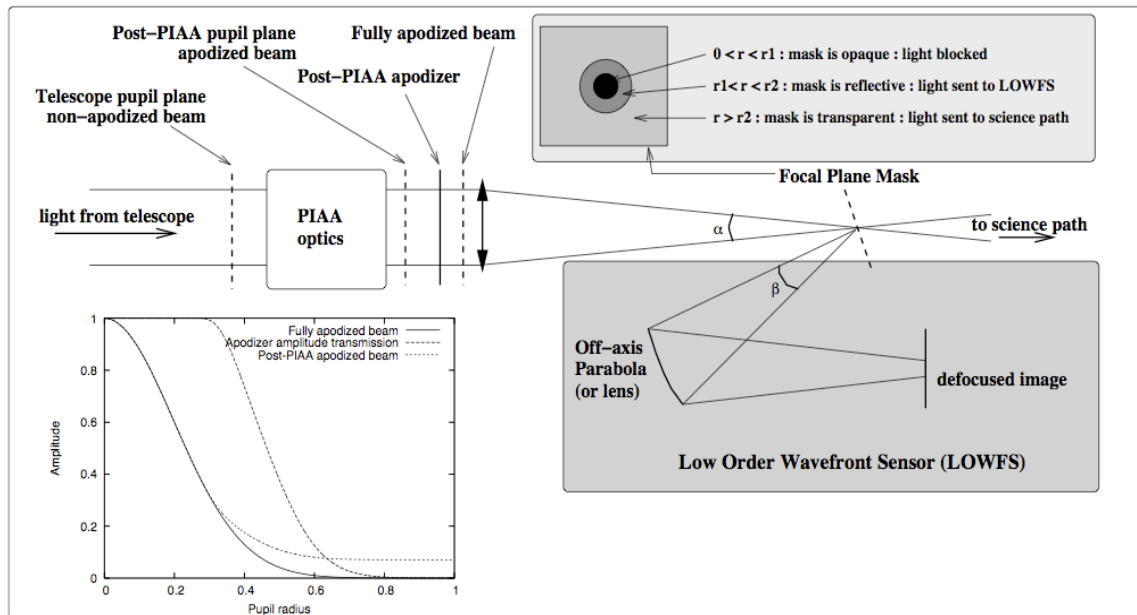


Figure A-1: LOWFS architecture. A dual zone focal plane mask extracts starlight from the focal plane to measure pointing.

LOWFS: principle

As shown in Figure A-1, the LOWFS uses starlight falling on the coronagraph focal plane mask: this light would otherwise be lost by the coronagraph. Thanks to a focal plane mask with a dark central zone surrounded by a reflective annulus, the LOWFS is insensitive to non-common path errors. The LOWFS performs a differential measurement between images: each image acquired by the LOWFS is compared to a reference image acquired during calibration, and this difference is linearly decomposed as a weighted sum of two modes, corresponding to the change due to tip and tilt motion. These modes are also acquired during calibration. The coefficients of the weighted sum are the tip and tilt measurements. Since the LOWFS uses the same camera for calibration and measurement, and since the measurement is differential, static errors in the camera (such as flat field error or bias) have no effect on the measurement. The large amount of incident

light on the focal plane mask allows fast (>100 Hz) and accurate ($< \text{mas}$) unbiased measurement of pointing.

Results obtained in LOWFS prototype at the Subaru testbed - relevance to proposed MAM chamber test and PECO

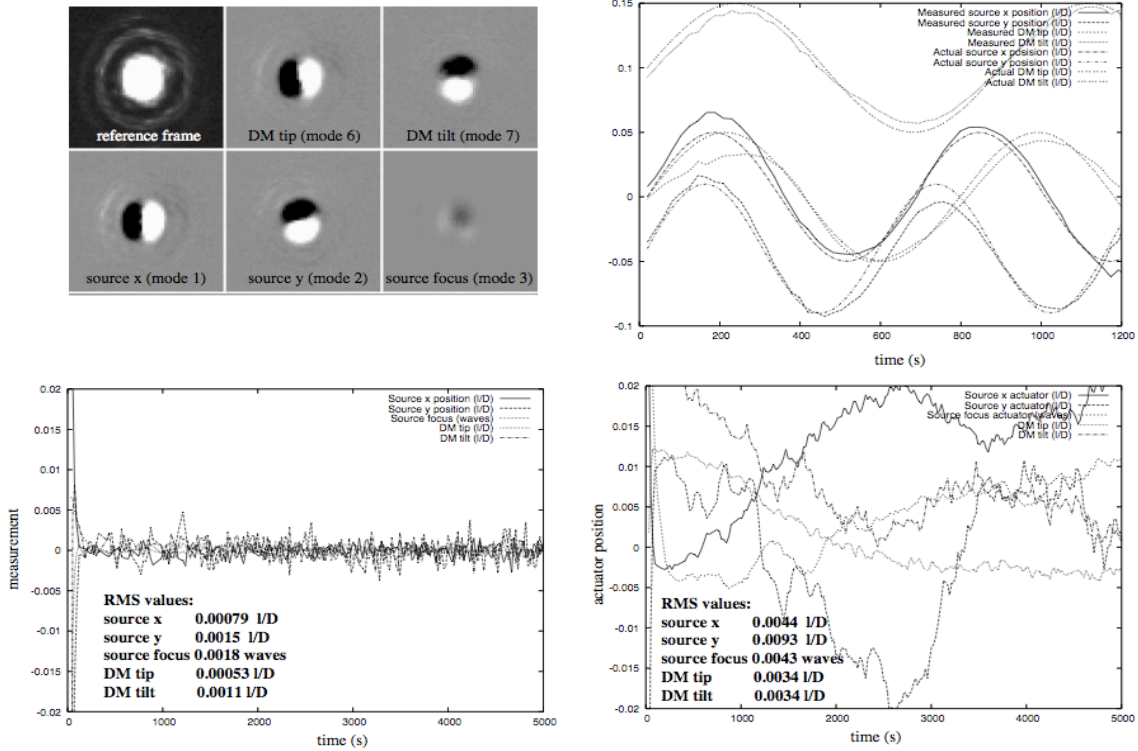


Figure A-2: Laboratory performance for the CLOWFS. Upper left: Measured CLOWFS reference frame and influence functions for the 5 axis controlled in the experiment. Pre-PIAA and post-PIAA modes look extremely similar (5% relative difference), and the signal must therefore be of high quality ($\text{SNR} > 20$) to properly identify these modes in a linear decomposition. Top right: Open loop simultaneous measurement of pre and post-PIAA modes. The measured amplitudes match very well the sine-wave signals sent to the actuators, and the CLOWFS is able to accurately measure all 4 modes shown here with little cross-talk. Since this measurement was performed in open loop, the measurement also includes unknown drifts due to the limited stability of the testbed. Bottom left: Closed loop measurement of the residual error for the 5 modes controlled. The achieved pointing stability is about $10^{-3} \lambda/D$ for both the pre-PIAA and post-PIAA tip/tilt. Bottom right: Position of the actuators during the same closed loop test.

Results obtained on the Subaru testbed with a LOWFS operating in visible light are summarized in Figure A-2, taken from [12]. The experiment was performed in air on a testbed which is not as stable as HCIT or MAM (or PECO). As shown in the lower left panel of Figure A-2, the source stability over 1-hr is approximately $0.01 \lambda/D$ RMS (1 mas on PECO). After closed loop correction, the source is maintained to about $0.001 \lambda/D$ RMS (0.1 mas on PECO) jitter with < 0.1 mas drift over one hour, which exceeds the requirements of our milestone, which is aimed at reproducing this achievement with increased calibration and a better controlled experiment.

Appendix B: The Pupil mapping Exoplanet Coronagraphic Observer (PECO)

The Pupil-mapping Exoplanet Coronagraphic Observer (PECO) mission concept uses a coronagraphic 1.4-m space-based telescope to both image and characterize extra-solar planetary systems at optical wavelengths. Figure B-1 shows the PECO spacecraft and telescope assembly. PECO can detect 10^{-10} contrast sources at $2 \lambda/D$ separation ($0.15''$) using a high-performance Phase-Induced Amplitude Apodization (PIAA) coronagraph which remaps the telescope pupil and uses nearly all of the light coming into the aperture. For exoplanet characterization, PECO acquires narrow field images simultaneously in 16 spectral bands over wavelengths from 0.4 to $0.9 \mu\text{m}$, utilizing all available photons for maximum wavefront sensing and sensitivity for imaging and spectroscopy. The optical design, shown in Figure B-2, is optimized for simultaneous low-resolution spectral characterization of both planets and dust disks using a moderate-sized telescope. PECO will image the habitable zones of about 20 known F, G, K stars at a spectral resolution of $R \sim 15$ with sensitivity sufficient to detect and characterize Earth-like planets and to map dust disks to within a fraction of our own zodiacal dust cloud brightness.

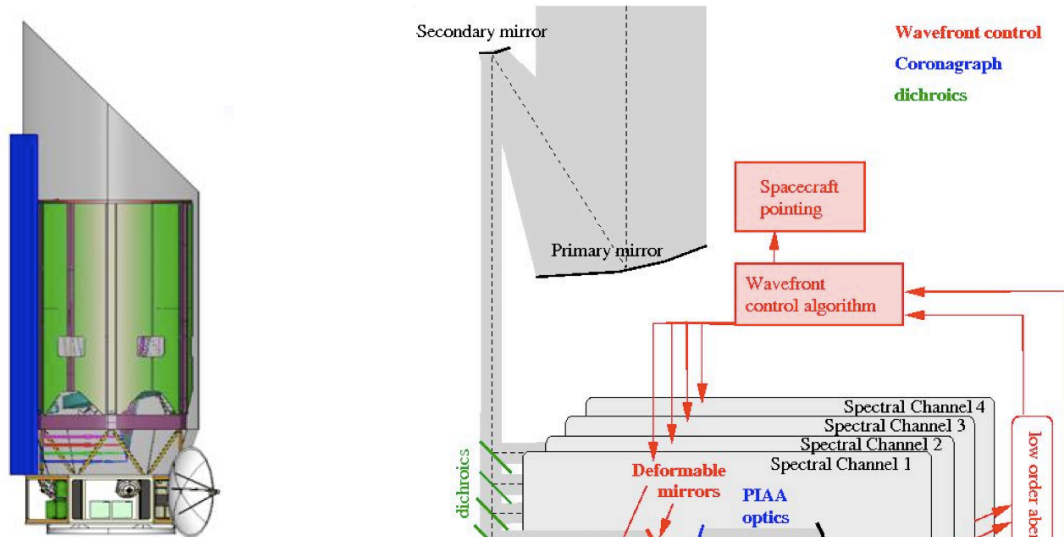


Figure B-1: PECO spacecraft and optical telescope assembly

Figure B-2: Baseline PECO coronagraph instrument architecture. Dichroics separate broadband (400nm - 900nm) light in 4 channels. Each channel includes its own PIAA coronagraph and wavefront control hardware, allowing all photons from 400nm to 900nm to be simultaneously used. Advances in polychromatic mask design and wavefront control may reduce the number of required channels.

A broad overview of the PECO mission can be found in the PECO team's report to astro2010 [2], available on http://caao.as.arizona.edu/PECO/PECO_Report.pdf.

Detailed information on the PECO mission can be found in the following documents:

- The PECO Science Requirements Document [15] available on:
http://caao.as.arizona.edu/PECO/PECO_SRD.pdf
- The PECO Design Reference Mission [16] available on:
http://caao.as.arizona.edu/PECO/PECO_DRM.pdf
- The PECO Technology Development Plan [17] available on:
http://caao.as.arizona.edu/PECO/PECO_techdev.pdf

The PIAA coronagraph requirements given in the next paragraph are derived from the PECO science requirements documents.

Appendix C: Pointing control on PECO

Requirements for PECO

- (1) The telescope pointing should be stable within 10 mas on hour timescales. This requirement is imposed by beam walk on optics, which, if pointing is not stable, will create speckles as pointing changes.
- (2) The instrument pointing tolerance during observations is no more than 1% of the diffraction width (i.e. <1 mas) to keep the pointing contribution to raw contrast at or below 10^{-9} . This requirement is imposed by photon noise sensitivity.
- (3) In addition to the pointing jitter requirement described above, the time-averaged position of the star image over the focal plane coronagraph mask should be stable (or known) to within 0.1mas over a period of a few hours to avoid coherent mixing of starlight leaks with residual speckles. This second requirement is imposed by calibration issues: detection of planets at the IWA of the coronagraph can easily be confused by small pointing offsets.

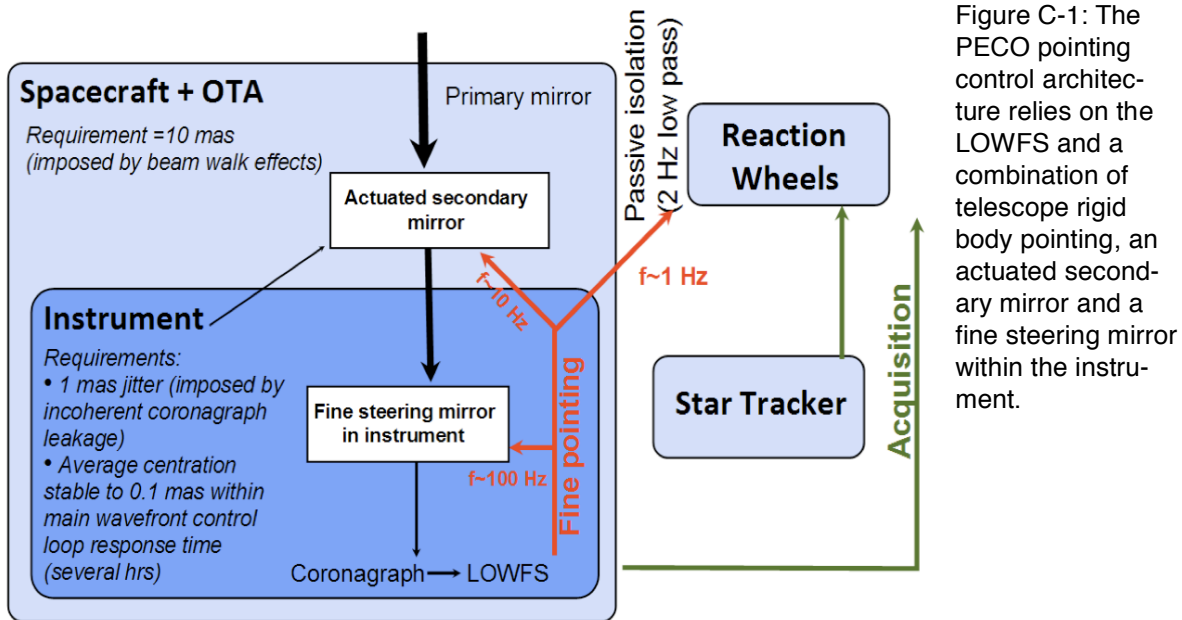


Figure C-1: The PECO pointing control architecture relies on the LOWFS and a combination of telescope rigid body pointing, an actuated secondary mirror and a fine steering mirror within the instrument.

Pointing control strategy on PECO

The PECO strategy to meet this stability is fourfold:

- 1) Operate in a very stable environment far from Earth (heliocentric orbit)
- 2) Eliminate vibration coupling from the reaction wheels by using a hexapod isolation system under each reaction wheel and design the OTA and optical mounting for stiffness
- 3) Derive an accurate control signal from the bright target star image reflected by the coronagraphic stop. The LOWFS measures sub-mas pointing errors at >100 Hz.,
- 4) Use the actuated telescope secondary mirror (momentum compensated) and fine steering the DMs conjugated to the pupil within the instrument to meet the tight instrument pointing tolerance (1 mas) with a relaxed OTA pointing requirement of 10 mas. Using HST as a bench-mark (<10 mas pointing stability in LEO), our models show we will meet the OTA pointing requirement.